Figure 3. Clinical correlation of serum CCN1 levels in SSc patients.

Serum CCN1 levels were measured by a specific ELISA. The levels were compared among dcSSc (n = 40), lcSSc (n = 26), and control subjects (n = 20) (a) and between SSc patients with digital ulcers (n = 24) and those without (n = 42) (b). Horizontal bars represent median of each group.

Figure 1

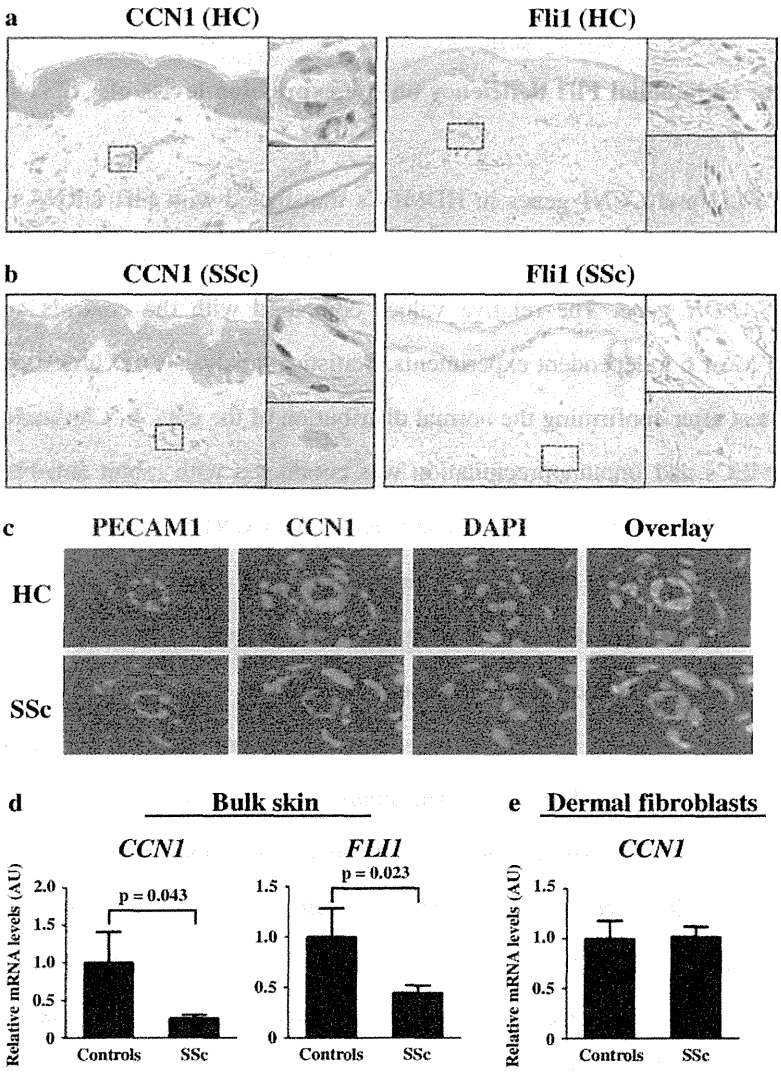

Figure 2

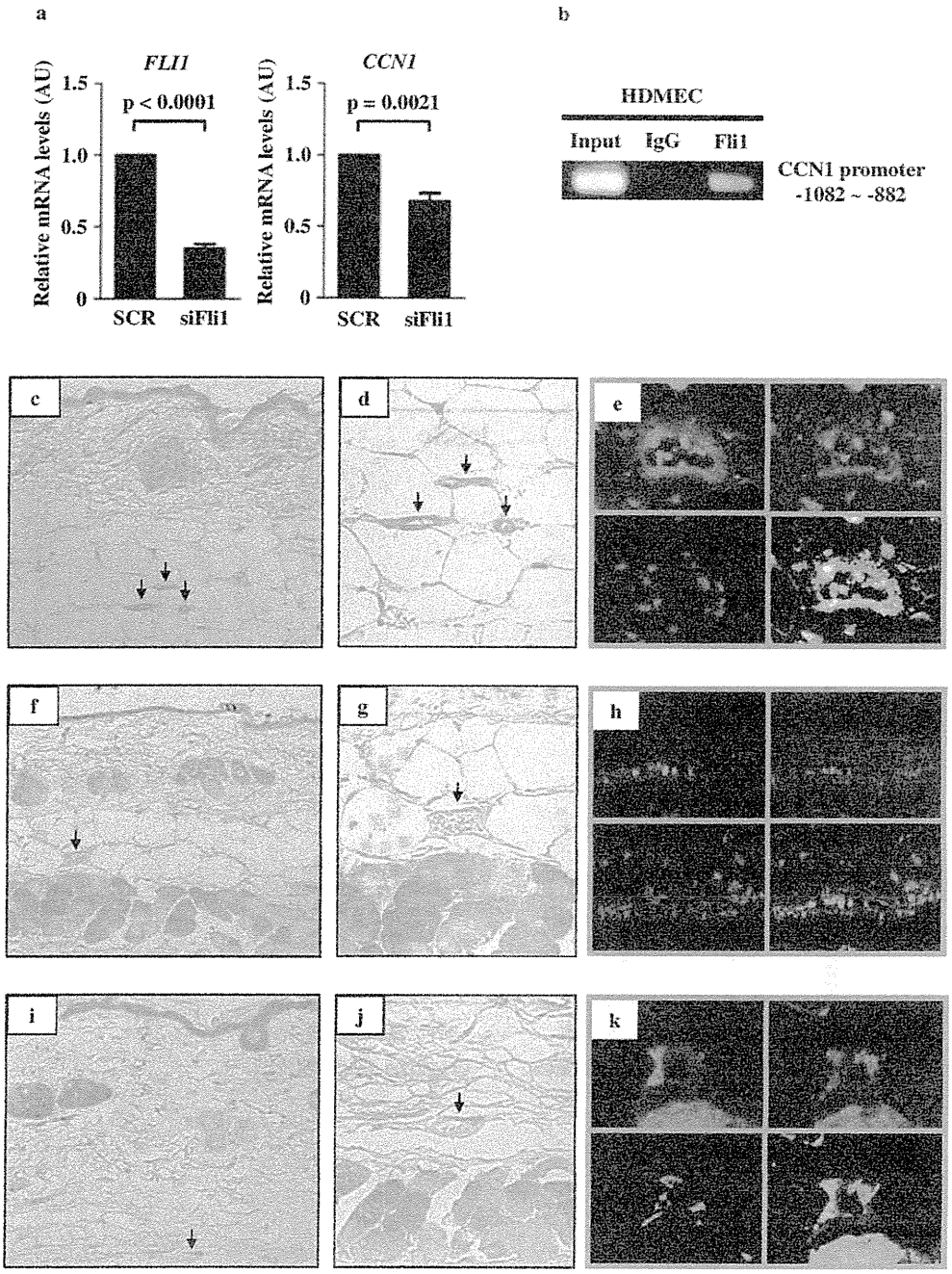

Figure 3

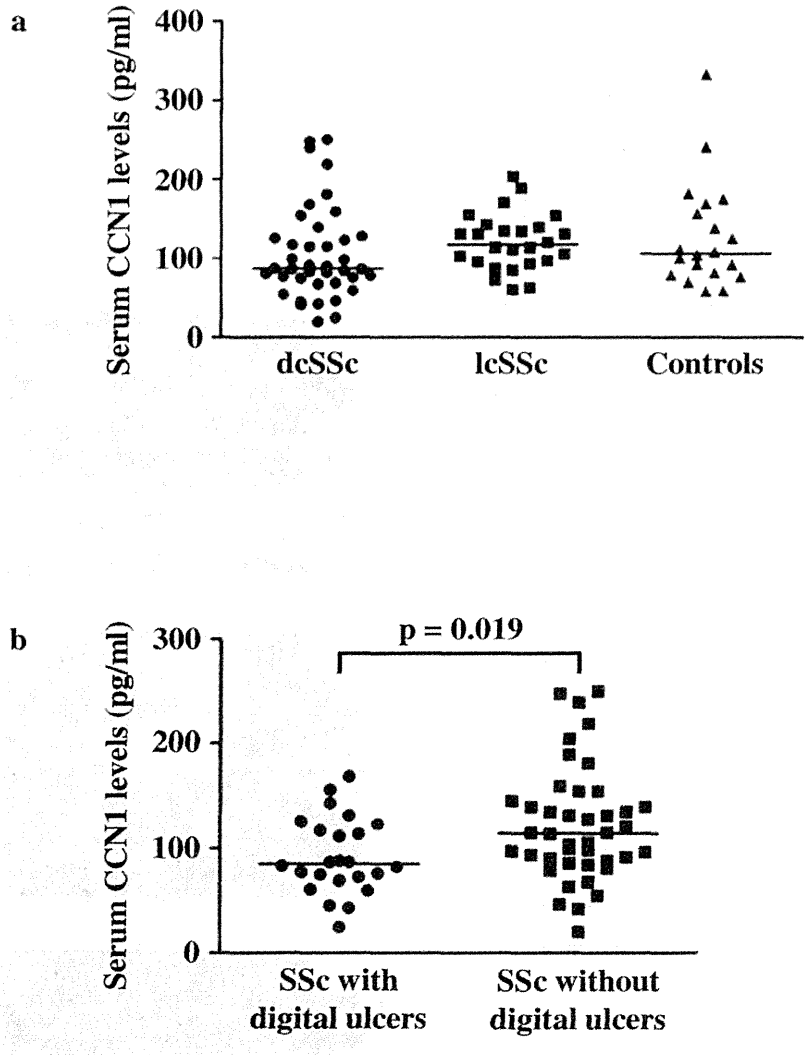

Full Length

Arthritis & Rheumatism
DOI 10.1002/art.38901

TLR4 knockout ameliorates tissue fibrosis in the murine models of systemic sclerosis

The running head: Impact of TLR4 loss on SSc murine models

Takehiro Takahashi, M.D., Yoshihide Asano, M.D., Ph.D., Yohei Ichimura, M.D., Tetsuo Toyama, M.D., Takashi Taniguchi, M.D., Shinji Noda, M.D., Ph.D., Kaname Akamata, M.D., Ph.D., Yayoi Tada, M.D., Ph.D., Makoto Sugaya, M.D., Ph.D., Takafumi Kadono, M.D., Ph.D., and Shinichi Sato, M.D., Ph.D.

Department of Dermatology, University of Tokyo Graduate School of Medicine, 7-3-1 Hongo, Bunkyo-ku, Tokyo 113-8655, Japan

Address correspondence to: Yoshihide Asano, M.D., Ph.D., or Shinichi Sato, M.D., Ph.D., Department of Dermatology, University of Tokyo Graduate School of Medicine, 7-3-1 Hongo, Bunkyo-ku, Tokyo 113-8655, Japan
TEL +81-3-5800-8661, FAX +81-3-3814-1503
E-mail: yasano-tky@umin.ac.jp or satos-der@h.u-tokyo.ac.jp

Funding source: This work was supported by Health Science Research Grants from the Ministry of Health Welfare and Labor of Japan, grants from Education, Culture, Sports, Science and Technology of Japan, and also by Grant-in-Aid for Japan Society for the Promotion of Science (JSPS) Fellows (to T.T.) (Grant No. 24-4204). The funders had no role in study design, data collection and analysis, decision to publish, or preparation of

Received: Nov 21, 2014; Revised: Aug 11, 2014; Accepted: Sep 30, 2014

the manuscript.

ABSTRACT

Objective: Bleomycin (BLM)-induced fibrosis model and tight skin mice (TSK/+) model are well-established experimental murine models of human systemic sclerosis (SSc). Growing evidence has demonstrated the pivotal role of Toll-like receptors (TLRs) in several autoimmune inflammatory diseases including SSc. The aim of this study is to determine the role of TLR4 in the fibrotic processes of these models.

Methods: We generated BLM-induced SSc murine model with $TLR4^{-/-}$ mice and $TLR4^{-/-}$;TSK/+ mice. The mechanisms by which TLR4 contributes to pathological tissue fibrosis were investigated utilizing these two models with histological examination, hydroxyproline assay, ELISA, real-time PCR, and flow cytometry.

Results: Dermal and lung fibrosis was attenuated in BLM-treated $TLR4^{-/-}$ mice compared with their wild type counterparts. Consistently, inflammatory cell infiltration, expression of various inflammatory cytokines, and pathological angiogenesis induced by BLM treatment were suppressed with TLR4 deletion. Furthermore, the increased expression of interleukin (IL)-6 in fibroblasts, endothelial cells, and immune cells in response to BLM *in vivo* and to LPS *in vitro* was remarkably abrogated in the absence of TLR4. Moreover, TLR4 deletion was associated with alleviated B cell activation and skew in Th2/Th17 response against BLM treatment. Importantly, also in TSK/+ mice, another SSc murine model, TLR4 abrogation attenuated its hypodermal fibrosis.

Conclusion: These results indicate the pivotal contribution of TLR4 to the pathological tissue fibrosis of SSc murine models. Our results indicate the critical role of TLR4 signaling in the development of tissue fibrosis, suggesting that biomolecular TLR4 targeting might be a potential therapeutic approach to SSc.

INTRODUCTION

Systemic sclerosis (SSc) is an autoimmune disorder characterized by initial vascular injuries and resultant fibrosis in the skin and certain internal organs (1). Numerous studies have shown that the complex interactions between leukocytes, endothelial cells, and fibroblasts lead to fibroblast activation and extracellular matrix overproduction (2). These interactions are mediated by several inflammatory cytokines, chemokines, growth factors and adhesion molecules. Interleukin (IL)-1, IL-4, IL-6, IL-13, IL-23, TNF-α, and MCP-1, are elevated in SSc patients' sera (3-6) and play critical roles in BLM-induced SSc mouse models as well (7, 8). Imbalance between Th1 and Th2 cytokines throughout the disease course of SSc further suggests the capital roles of these factors (9). Th2 polarization is characteristic of early diffuse cutaneous SSc (dcSSc), while the balance shifts to Th1 predominance along with the resolution of skin sclerosis, and persistent Th2 predominance is related to poor prognosis (10). Among these factors, IL-6 has drawn attention as a new therapeutic target. IL-6 blockade attenuates skin sclerosis induced by bleomycin (BLM) in animal models (11) and tocilizumab, an anti-IL-6 receptor monoclonal antibody, improves dermal sclerosis in a subset of SSc patients (12). Supporting this notion, the contribution of Th17 subset, whose differentiation is regulated by IL-6, is recently reported (13).

Researches have disclosed the role of innate immunity in the pathogenesis of autoimmune diseases including SSc (14). Innate immune response is mediated, in part, by Toll-like receptors (TLRs), which are evolutionarily conserved receptors for foreign pathogen-associated molecular patterns (15). TLRs and their ligands contribute to inflammatory responses including autoimmune diseases as well as host defenses by innate immunity (16), and they further control adaptive immune responses (17).

Microbial TLR ligands trigger onset in experimental models of arthritis, diabetes, and atherosclerosis (18). Furthermore, various endogenous molecules serve as ligands for TLRs. TLR4, originally identified as the receptor for lipopolysaccharide (LPS), recognizes hyaluronic acid (HA), fibronectin fragments, heparan sulfate, and High-Mobility Group Box-1 (HMGB-1) as endogenous ligands (18). This recognition is profoundly related to the persistent inflammatory and/or fibrotic process in collagen diseases (19).

In SSc patients, serum levels of HA and HMGB-1, and expression of HA in lesional skin are elevated (20-22). TLR4 stimulation by these molecules results in fibroblast activation by augmenting TGF-β signaling (22). Importantly, in C3H/HeJ mice with point mutations in *Tlr4* gene, BLM-induced skin sclerosis is attenuated despite the elevation of endogenous TLR4 ligands (22). These results indicate that TLR4 signaling activation is potentially involved in the fibrotic process of SSc and its animal models at least partly by directly activating dermal fibroblasts. However, given that C3H/HeJ mice exhibit several defects including spontaneous alopecia development caused by some unknown immunological abnormalities (23), the exact role of TLR4 in the pathological process of tissue fibrosis still remains unknown. Therefore, we generated BLM-treated and tight skin mice with TLR4 deletion and investigated the significance of TLR4 in these models. Our results indicate the critical role of TLR4 signaling in the development of tissue fibrosis in these models, suggesting that biomolecular TLR4 targeting is a potential therapeutic approach to SSc.

MATERIALS AND METHODS

Mice.

Wild type (WT) (C57BL/6) mice were purchased from Japan SLC Inc. (Tokyo, Japan). $TLR4^{-/-}$ and TSK/+ mice (C57BL/6 background) were purchased from The Jackson Laboratory. $TLR4^{-/-}$;TSK/+ mice were generated by crossing TSK/+ and $TLR4^{-/-}$ mice. All mice used in this study were female, and in BLM-treated model, mice were 6 to 8 weeks old at the beginning of the PBS/BLM treatment. In the experiments with TSK/+ mice, they were sacrificed at 8-week-old time point and skin and lung sections were excised for histological evaluations.

BLM treatment.

BLM (Nippon Kayaku, Tokyo, Japan) was prepared and injected to mice as described previously (24). For histological analysis to evaluate fibrosis, alternate-day injection for 3 weeks, and for analysis of inflammatory cell infiltration, neovascularization, cytokine expressions, and flow cytometry, daily injection for 1 week was made in each group, otherwise indicated. Equal volume of PBS was injected to control groups. All studies and procedures were approved by the Committee on Animal Experimentation of University of Tokyo Graduate School of Medicine.

Histological assessment and immunohistochemistry.

On the next day of the final injection, mice were sacrificed, and skin and lung sections were taken. Six-μm thick sections were stained with H&E, Masson's trichrome and toluidine blue. Dermal and hypodermal thickness was examined as previously described (13, 25). Right lungs were excised, and the severity of fibrosis was scored as previously described (25). Immunohistochemistry was performed using antibodies directed against TLR4 (Imgenex, San Diego, CA, USA), CD3 (BD Pharmingen, San Diego, CA, USA),

B220 (BD Pharmingen), F4/80 (Serotec, Eching, Germany), α-smooth muscle actin (α-SMA) (Sigma-Aldrich, St. Louis, MO, USA), CD31 (BD Pharmingen) and IL-6 (Abcam, Cambridge, UK). For immunofluorescence staining, serial sections were incubated with antibodies against TLR4, α-SMA, CD31, and HA (Abcam) as primary antibodies, followed by Alexa Fluor 555 or fluorescein isothiocyanate (FITC)-conjugated secondary antibodies (Abcam) corresponding to their primary antibodies. Coverslips were mounted using Vectashield with DAPI (Vector Laboratories, Burlingame, CA), and staining was examined with Bio Zero BZ-8000 (Keyence, Osaka, Japan). Stained cells were counted in 10 random grids under high-magnification power fields by two independent researchers (T.T. and Y.A.) with blinded manners.

Collagen measurement.

Collagen contents of skin and lung tissues were quantified following the instructions of QuickZyme Total Collagen Assay (QuickZyme Biosciences, Leiden, Netherlands). Six-mm punch biopsy skin samples and total left lungs were used.

Measurement of cytokines in sera and skin homogenates.

Sera of mice were obtained after 3-week treatment with PBS/BLM. Serum total IgG, IgM, anti-DNA topoisomerase I antibody, and IL-6 levels were determined by specific ELISA kits (IL-6: R&D Systems, Minneapolis, MN, USA; total IgG and IgM: Abcam; anti-DNA topoisomerase I antibody: ALPHA DIAGNOSTIC, San Antonio, TX, USA)

following manufacturer's instructions. Six-mm punched out lesional skin of mice treated with either PBS or BLM for 1 week was harvested, homogenized in 300 μl of RIPA buffer (Santa Cruz Biotechnology, Santa Cruz, CA, USA) and centrifuged. Lysates were subject to measurement with specific ELISA kits for IL-6, IL-13, and IL-17A (R&D Systems).

RNA isolation and real-time (RT) PCR.

One μg of RNA was reverse transcribed using iScript cDNA Synthesis Kits (Bio-Rad, Hercules, CA, USA). RT-PCR was carried out using SYBR Green PCR Master Mix (Life technologies, Gaithersburg, MD, USA) on ABI prism 7000 (Life technologies) in triplicates. The mRNA levels were normalized to those of GAPDH gene. The primer sequences used are available upon request. The relative change in the levels of genes of interest was determined by the $2^{-\Delta\Delta CT}$ method. Dissociation analysis for each primer pair was performed to verify specific amplification.

Cell isolation and culture.

Dermal fibroblasts were purified as descried previously (26). Primary WT and $TLR4^{-/-}$ fibroblasts were passaged once and utilized for experiments. To obtain dermal microvascular endothelial cells, cell suspension obtained from dermal collagenase digestion was stained with anti-CD31 microbeads (Myltenyi Biotech, Bergisch Gladbach, Germany), and isolated with magnetic sorting, as described previously (27). WT or $TLR4^{-/-}$ primary fibroblasts or endothelial cells were seeded 3×10^4 cells per well, stimulated with 100 ng/ml LPS from E.coli (Sigma-Aldrich) for 24 hours, to evaluate

supernatant IL-6 concentration with specific ELISA kit (R&D systems). Macrophages were obtained as described previously (28). Splenic B cells and T cells were isolated with anti-CD19 MACS magnetic beads and pan-T cell isolation kit, respectively (Miltenyi Biotech). Five × 10^4 cells per well were stimulated with 100 ng/ml LPS or left untreated. Supernatants were harvested 24 hours later and measured for IL-6 concentration with specific ELISA kit (R&D systems). In experiments to determine IL-4, IL-6 and TGF-β1 productions by purified B cells from PBS or BLM-treated mice, mice were treated for 1 week, sacrificed, and cells from the draining lymph nodes (i.e. axillary and inguinal lymph nodes) of the lesional skin were subject to magnetic separation with anti-CD19 MACS beads. The CD19 positive cells were cultured in RPMI medium without stimulation and after 24 hours, supernatants were harvested and above cytokines were measured with specific ELISA kits (R&D systems).

Flow cytometric analysis.

Mice were treated with PBS/BLM for 1 week. On the next day of the final injection, lymphocytes from draining lymph nodes were obtained. In the surface staining experiments, cells were stained with antibodies against B220 (RA3-6B2), CD3 (17A2), F4/80 (BM8), CD11c (N418) and TLR4 (SA15-21; all from Biolegend, San Diego, CA, USA). In intracellular cytokine staining, they were stimulated with 10 ng/ml PMA and 1 μg/ml ionomycin (Sigma-Aldrich) in the presence of 1 μg/ml brefeldin A (GolgiStop; BD Pharmingen) for 4 hours. Cells were washed, stained for CD4, treated with fixative/permeabilization buffer (BD Pharmingen) and then stained with anti-IL-4 (11B11), anti-IL-17A (TC11.18H10) and anti-IFN-γ (XMG1.2; all from BioLegend) antibodies. In experiments to analyze transcription factors, antibodies against ROR-γt

(B2D; eBioscience, San Diego, CA, USA), T-bet (4B10; Biolegend), and Foxp3 (FJK-16s; eBioscience) were used. Cells were analyzed on a FACSVerse flow cytometer (BD Biosciences, San Jose, CA, USA). The positive and negative population of cells were determined using unreactive isotype-matched antibodies as controls.

Statistical analysis.

Data are presented as mean ± SEM. Statistical analysis was carried out using GraphPad Prism with two-tailed Mann-Whitney U test for group comparisons. $P < 0.05$ was considered statistically significant.

RESULTS

TLR4 and its endogenous ligand expressions are enhanced by BLM treatment.

We initially evaluated TLR4 expression after the BLM treatment in WT mice. Immunohistochemical staining of the lesional skin and the lung revealed a significant increase in TLR4 positive cells (Fig. 1A and B). Since the expression of TLR4 is increased in α-SMA positive cells and CD31 positive dermal microvascular endothelial cells in the lesional skin of SSc patients (22), we performed double immunofluorescence staining to clarify if TLR4 expression is increased in these cells as well in BLM-treated mice. As shown in Fig. 1C, we noted prominently enhanced TLR4 expression in α-SMA and CD31 positive cells, together with increased number of these cells in BLM-treated mice compared with control mice. Indeed, 61.8 ± 14.2% and 25.6 ± 8.5% of TLR4-positive interstitial cells in the BLM-treated mice were also positive for α-SMA and CD31 respectively, indicating robust TLR4 expression in myofibroblasts and endothelial cells. We further examined whether these α-SMA

positive cells could express endogenous ligands such as HA, with double staining of HA and α-SMA. Indeed, the result revealed marked colocalization of these two molecules (Fig. 1C).

We next performed flow cytometric analysis with cells isolated from draining lymph nodes of the lesional skin. Although no difference was seen in dendritic cells, enhanced TLR4 expression was observed in B cells, T cells, and macrophages in BLM-treated mice (Fig. 1D). These results indicate that BLM increases the expression of TLR4 in various cell types as well as that of endogenous TLR4 ligands in the lesional skin.

TLR4 deletion attenuates skin fibrosis, inflammatory cell infiltration, and angiogenesis in BLM-treated mice with decreased pro-fibrotic cytokine expression. To evaluate the effect of TLR4 loss on skin fibrosis, lesional skin sections of mice treated with PBS/BLM for 3 weeks were assessed. As shown in Fig. 2A, the dermal thickness and collagen content were reduced in BLM-treated $TLR4^{-/-}$ mice compared with BLM-treated WT mice, and the increase in α-SMA positivity was also attenuated by TLR4 deletion (Fig. 2A). B cell, T cell, macrophage, and mast cell infiltration showed marked increase by BLM injection in WT mice, while $TLR4^{-/-}$ mice showed milder infiltration (Fig. 2B). In addition, CD31 staining revealed increased vessels in the deep dermis and subcutaneous fat tissue of BLM-treated WT mice, while TLR4 knockout attenuated the increase (Fig. 2B). Collectively, these results indicate that the activation of TLR4 signaling plays vital roles in the pathogenic fibrotic processes including inflammatory cell infiltration and angiogenesis caused by BLM.

We next explored the expression profiles of mRNAs in the lesional skin. BLM

treatment increased the mRNA levels of *Il1b*, *Il6*, *Il13*, *Il17a*, *Il23a*, *Tnf*, *Ifng*, *Tgfb1*, *Ccl2*, *Icam1*, *Vcam1*, and *Sele* genes in WT mice, and the increased levels of these mRNAs were suppressed by TLR4 deletion (Fig. 2C). Protein levels in the lesional skin showed significantly less expression of IL-6, IL-13, and IL-17A in BLM-treated TLR4$^{-/-}$ mice compared with WT mice (Fig. 2D). These results indicate that TLR4 is a key molecule required for the expression of soluble factors and cell adhesion molecules which coordinately regulate tissue fibrosis in BLM-induced SSc model.

Fibrosis and expression of inflammatory cytokines are reduced in the lungs of BLM-treated TLR4$^{-/-}$ mice.

In addition to skin sclerosis, this murine model accompanies lung fibrosis. Histological analyses revealed less fibrosis and inflammatory cell infiltration in BLM-treated TLR4$^{-/-}$ mice than in BLM-treated WT mice (Fig. 3A and B). In parallel with the results in the skin, the mRNA levels of the *Il1b*, *Il6*, *Il13*, *Il23a*, *Tnf*, *Ccl2*, and *Sele* genes were significantly suppressed in BLM-treated TLR4$^{-/-}$ mice compared with BLM-treated WT mice (Fig. 3C), and the levels of *Il17a and Tgfb1* were tended to be suppressed by TLR4 deletion ($p = 0.09$ and $p = 0.06$, respectively; Fig. 3C). These results indicate that TLR4 signaling plays a pivotal role in pulmonary fibrosis as well by regulating the expression of various soluble factors, growth factors and cell adhesion molecules in BLM-induced SSc model.

Serum IgG, anti-DNA topoisomerase I antibody and IL-6 levels are reduced by TLR4 knockout with attenuated expression of IL-6 in the lesional skin and *in vitro*.

We next proceeded to examine the serum total IgG, IgM, anti-DNA topoisomerase I

antibody, and IL-6 levels to evaluate the systemic immunological influence of TLR4 deletion in this murine model. In line with other observations, serum total IgG and IL-6 levels were significantly decreased, and anti-DNA topoisomerase I antibody level was tended to be decreased ($p = 0.06$) in BLM-treated TLR4$^{-/-}$ mice compared with their WT counterparts (Fig. 4A). Considering the pivotal role of IL-6 in the fibrotic process in this disease model as well as in SSc through its direct pro-fibrotic property and immunomodulatory role (29), we next focused on this molecule. IL-6 immunostaining in the lesional skin showed increased expression in fibroblasts, endothelial cells, and perivascular inflammatory cells in BLM-treated WT mice, while the expression was suppressed in their TLR4$^{-/-}$ counterparts (Fig. 4B). To clarify the impact of TLR4 loss on IL-6 production, we isolated and stimulated respective cells, which are potentially responsible for the decreased IL-6 production in TLR4$^{-/-}$ mice, namely fibroblasts, endothelial cells, and inflammatory cells, such as macrophages, B cells, and T cells. LPS stimulation of these cells from WT mice resulted in a marked increase in IL-6 production in the culture supernatants, while TLR4 deletion strikingly suppressed its production (Fig. 4C). These results suggest that TLR4 activation in various cell types by endogenous ligands induced by BLM might promote tissue fibrosis in skin and lung at least partly through IL-6 production, which was abrogated by TLR4 deletion.

B cell activation and polarization towards Th2/Th17 induced by BLM treatment are attenuated in TLR4$^{-/-}$ mice.

Above observations on serum IgG and anti-DNA topoisomerase I antibody encouraged us to examine systemic immunological impact of TLR4 loss on lymphocytes in this disease model. We first noticed increased number of cells in lesional lymph nodes of

WT mice treated with BLM for 1 week, while BLM treatment in TLR4$^{-/-}$ mice caused no remarkable change (Fig. 5A). B cells purified from lymph nodes of BLM-treated WT mice exhibited enhanced pro-fibrotic cytokine (IL-4, IL-6, and TGF-β1) production, while B cells from their TLR4$^{-/-}$ counterparts showed lower production, indicating attenuated activation of B cells in TLR4$^{-/-}$ mice (Fig. 5B). We then proceeded to assess Th1/Th2/Th17 environment of these diseased mice. Evident polarization towards Th2/Th17 in CD4^{+} T cells was confirmed by the increased intracellular expression of IL-4 and IL-17A in WT mice. However in TLR4$^{-/-}$ mice, the increase was attenuated, while the induction of IFN-γ was comparable (Fig. 5C and D). We further evaluated master regulators of CD4^{+} T cell differentiation, such as RAR-related orphan receptor γT (ROR-γt) for Th17, T-box expressed in T cells (T-bet) for Th1, and Forkhead box p3 (Foxp3) for regulatory T cells. In line with above observations, while ROR-γt expression was significantly increased in WT mice with BLM treatment, there was no increase in ROR-γt expression in TLR4$^{-/-}$ mice. T-bet expression was increased by BLM treatment both in WT and TLR4$^{-/-}$ mice, but to a significantly greater extent in TLR4$^{-/-}$ mice. Foxp3 expression was comparable between BLM-treated WT and TLR4$^{-/-}$ mice (Fig. 5D). Thus, these results indicate that TLR4 signaling is indispensable in the context of B cell activation and Th2/Th17 skewed polarization in BLM-induced SSc model.

Hypodermal fibrosis in TSK/+ mice is attenuated by TLR4 knockout.

To further explore the impact of TLR4 knockout in another SSc murine model, we crossed TLR4$^{-/-}$ mice with TSK/+ mice, a genetic SSc murine model which is primarily characterized by endogenous activation of fibroblasts (30), generating TLR4$^{-/-}$;TSK/+

mice. Histological assessment of hypodermal thickness, the thickness of the subcutaneous loose connective tissue layer, revealed significantly decreased thickness in TLR4$^{-/-}$;TSK/+ mice compared with control TSK/+ mice (Fig. 6A). In contrast to this observation, emphysematous changes in the lungs of TSK/+ mice were not influenced by TLR4 deletion (Fig. 6B). These results suggest the critical roles of TLR4 signaling also in TSK/+ model along with BLM-induced model, further indicating its importance in pathological tissue fibrosis.

DISCUSSION

Extensive studies have shown that TLR4 is involved in fibrotic processes (31). This study was undertaken to clarify the contribution of TLR4 signaling to the pathological fibrosis of SSc murine models.

The pathological influence of TLR4 upregulation has been shown in various chronic inflammatory diseases, and increased TLR4 signaling alone can break immunological tolerance (32). However, in the field of SSc research, the pathogenic interest of TLR4 has been put on the activation of dermal fibroblasts via their own TLR4 signaling. In this study, in line with the observation that approximately 50% and 25% of TLR4-positive interstitial cells in the SSc lesional dermis were also positive for α-SMA and CD31, respectively (22), our observation also revealed robust TLR4 upregulation in α-SMA and CD31 positive cells, and we further demonstrated the enhanced TLR4 expression in the immune cells from BLM-treated mice. Furthermore, we detected enhanced HA production by α-SMA positive cells which might primarily be myofibroblasts. Using lung fibrosis model induced by BLM, Li et al. showed that this fibrosis is caused by the activated myofibroblasts which actively produce HA (33).

Taken together, our results suggest that BLM induces TLR4 activation along with enhanced production of endogenous TLR ligands from these activated cells, and the positive autocrine/paracrine loop which is mediated by TLR4 might be involved in the pathogenesis of fibrosis in this model.

Our study showed reduced expressions of pro-fibrotic mediators in BLM-treated TLR4$^{-/-}$ mice. Previous studies have shown that IL-1β, IL-6, IL-13, IL-17A, TNF-α, TGF-β1, MCP-1, ICAM-1, VCAM-1, and E-selectin play essential roles in the pathogenesis of this disease model as well as SSc (7, 8, 11, 13, 24), and their expression levels were significantly decreased by TLR4 deletion. In addition, infiltration of B cells, T cells, macrophages, and mast cells plays important roles in this model as well as in SSc (34-36). TLR4 knockdown attenuated infiltration of these cells, and furthermore, suppressed dermal angiogenesis. Since aberrant angiogenesis is also an important disease process of SSc and its murine model (37), it is consistent to observe decreased angiogenesis in TLR4$^{-/-}$ mice with less fibrosis. In aggregate, the present study indicates the critical role of TLR4 to induce the pathological expression profiles of various soluble factors and cell adhesion molecules and pathological angiogenesis, which coordinately regulate tissue fibrosis in BLM-induced murine model and possibly in human SSc.

B cell activation is also a key factor that contributes to the pathogenesis of SSc and its murine models. In addition to the observation in mice that CD19 knockout attenuates BLM-induced skin and lung fibrosis (25), recent clinical observations that rituximab, an anti-CD20 antibody, is effective against skin and lung fibrosis in a certain subset of SSc (38), have proven the importance of B cells in SSc. Our observations that TLR4 abrogation alleviated increased levels of serum total IgG, anti-DNA

topoisomerase I antibody, and pro-fibrotic cytokine production by B cells in BLM-treated mice suggest the significance of TLR4-dependent B cell activation in the development of pathological fibrosis.

IL-6 is a classic pro-fibrotic cytokine which plays pivotal roles in the pathogenesis of SSc and its murine model (11, 29), and is produced by various cells including fibroblasts, endothelial cells, B cells, T cells and macrophages (39). IL-6 enhances collagen synthesis via promoting myofibroblastic differentiation (11). Furthermore, IL-6 drives $CD4^+$ T cells into IL-4-secreting Th2 cells while inhibiting Th1 differentiation and amplifying the pro-fibrotic response (40). In our experiments, reduced IL-6 levels were observed in BLM-treated $TLR4^{-/-}$ mice. The first step of the fibrotic process might include the generation of TLR4 endogenous ligands including HA by BLM treatment and their autocrine and/or paracrine recognition by TLR4 expressing cells. This recognition immediately stimulates these cells and enhances the production of this key cytokine, IL-6, and thus skewing Th1/Th2 balance towards Th2 predominance. Our *in vitro* data with LPS stimulation showed striking upregulation of IL-6 in various cell types (e.g. over 100-fold increased induction in macrophages), while there was only modest increase in IL-6 levels by BLM treatment *in vivo*. This discrepancy could be explained by the relatively weak but sustained impact of these endogenous ligands on inflammatory cytokine production relative to LPS, the extremely strong external ligand (41). Importantly, we observed that, in BLM-treated $TLR4^{-/-}$ mice, the degree of reduction in fibrosis was in parallel with the reduction of IL-6 expression, both of which are roughly a half the levels compared with their WT counterparts. Therefore, through its direct and indirect impacts on fibrosis, IL-6 might serve as an indicator of TLR4-dependent fibrotic activity. Further exploration on the role and the